

Effect of mechanical alloying on the properties of AA6005A/TiB MMC

M.V. Utrilla *, N. Abuwarda, M.D. Escalera, E. Otero, M.D. López

Dpto. de Matemática Aplicada Ciencia e Ingeniería de Materiales y Tecnología Electrónica, ESCET,
Rey Juan Carlos University, C/ Tulipán s/n, 28933, Móstoles (Madrid, Spain)

* victoria.utrilla@urjc.es

Keywords: Mechanical alloying (MA), Aluminium, Titanium boride, Metal matrix composite.

Abstract

An A6005 aluminium alloy composite reinforced with 5% titanium boride particles have been produced by P/M processing. As first step aluminium and titanium boride powders have been blended by mechanical alloying (MA). The samples obtained after MA processing were tested by scanning electron microscopy (SEM), laser diffraction spectroscopy (LDS), optical microscopy (OM) and X-ray diffraction (XRD) techniques to analyse particle microstructure, morphology and distribution. Also, to evaluate the blended powder mechanical properties, micro-hardness tests were performed. After 8 hours of mechanical alloying, the best size distribution and good mechanical properties were obtained as the steady state is reached.

1. Introduction

Properties shown by metal matrix composite materials [1], like high specific module, strength and thermal stability, make them interesting for aerospace applications and transport industry, especially for structural elements [2]. Those properties can be improved with the matrix and reinforcement (normally ceramic) grain size decrease [3-5].

Aluminium matrix composites reinforced with ceramic particles as silicon carbide (SiC), or titanium boride (TiB₂) [6-8], are considerably interesting because offer versatility regarding to the manufacture process and semi-isotropic properties compared with fibre reinforcements. These composites present high strength and stiffness, creep and wear resistance and in addition, good thermal and electrical conductivity. Titanium boride is especially attractive because shows high elastic module, strength, hardness and high thermal conductivity [9]. Also, it has an elevated melting point and great chemical stability. Besides, it is compatible with aluminium alloys and does not react with these at low temperatures. For this type of reinforcement, interfacial fragile products formation between matrix and reinforcement is avoidable [10]. In other hand, A6005 aluminium alloy could be a perfect candidate to be employed as matrix because in addition to its low cost and optimal properties, also has high corrosion resistance and good capacity to be extruded and welded.

In the last years, coinciding with the developing of metal matrix composite materials, new processes based in milling the separated alloy elements are coming up as good methods to obtain both alloys which are difficult to process by other methods and composite powders. Of these, one of the most effective and most interesting techniques is the MA [11-13]. It has demonstrated to be the most favourable technique to obtain pre-alloyed powders, due to the possibility to obtain compositions, properties and reinforcement distributions difficult to obtain by other methods, including atomization. In addition MA is not performed at high temperature which avoids problems during manufacturing and reduces costs.

The chief objective of this study is to search the best MA time through composite material characterization: microstructural changes, particles size and reinforcement distribution, with its corresponding change in properties. The purpose of future investigations is the compacting of the milled particles by hot extrusion to produce bulk nanostructured composite.

2. Experimental Procedure

A6005 aluminium alloy powders were used as matrix, with an initial particle size about 30 μm . The composition is shown in Table 1. Titanium boride powders were used as reinforcement with an average size between 30 and 50 nm. MA was carried out mixing the aluminium powders with 5wt% of reinforcement in an attritor mill (AIMEN Technological Centre). Samples were extracted every 60 minutes up to 10 hours of milling. The ball-to-powder weight ratio was 10:1. Balls diameter was 5 mm. The milling is performed in a cyclical operation mode with variable speed from 500 rpm (4 minutes) to 300 rpm (1 minute). In addition 3wt% of methanol was added as process control agent (PCA).

Al	Si	Fe	Mg	Cu	Mn	Cr	Zn	Ti	Mn+Cr
Bal.	0.88	0.18	0.57	0.11	0.13	0.01	0.11	0.10	0.14

Table 1. Chemical composition of A6005 aluminium alloy powders (weight percent).

XRD technique was used to determine crystal size in each sample using $K\alpha\text{Cu}$ ($1,54056\text{\AA}$) as radiation source with 45kV and 40mA as voltage and intensity respectively. LDS was used to analyse particle size. Powder microstructure and morphology has been studied with OM, SEM and FE-SEM. Microstructure of the samples has been revealed by attack with *Kellers* reactive. Hardness has been measured applying a load of 0.01 HV during 15 seconds. To obtain good precision in hardness values 16 measurements were performed for each sample and outliers were discarded from the population with Grubbs test.

3. Results

3.1. Base Material Characterization

Size, morphology and composition of the TiB_x nanoparticles were analysed before milling. As it can be seen in Figure 1, nanoparticles size is between 30 and 50 nm and have spherical shape, but present agglomerates of up to 1 μm . Nanoparticles composition was analysed by XRD where TiB and TiB_2 phases were revealed. TiB characteristic peaks are much more intense than TiB_2 peaks which meaning TiB is the major phase.

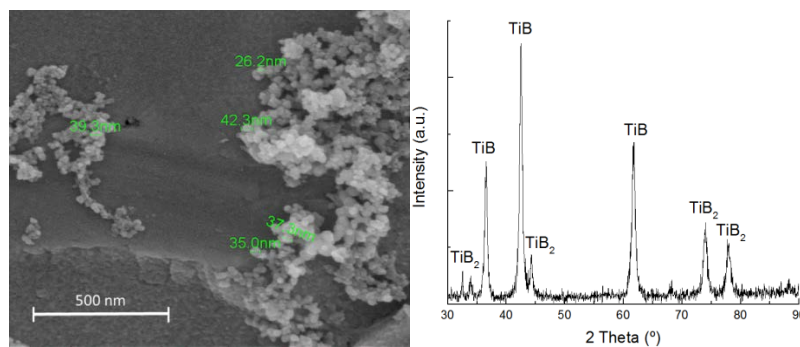


Figure 1. TiB_x nanoparticles: Size, distribution and XRD analysis.

3.2. Morphology and Particle Size

The most commonly used method of describing particle size distributions are D values. The D10, D50 (average) and D90 are used to represent the midpoint and range of the particle sizes of a given sample. Figure 2 represents particles size distribution measured by LDS. It shows progressive particle size decrease from 4 hours of milling for the midpoint (47.1 μm) and both particle size ranges, being more pronounced for the biggest range. This decline reaches a minimum at 8 hours of milling (16.6 μm for the midpoint); at this time it starts to increase.

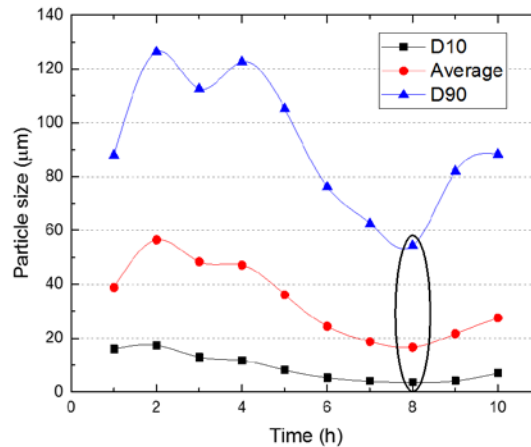


Figure 2. A6005/TiB_x particles size evolution at different MA times.

Particle size and morphology were also studied by SEM. As shown in Figure 3(a), powder particles milled during 1h present the original spherical morphology together with other powders which have begun to deform. This deformation is due to the impacts with balls and mill walls. In these step, the main mechanism is particles cold welding. It can be seen an important increment of powders size from 30.9 μm without milling to 38.8 μm after an hour. With increasing milling time, number of spherical particles starts to reduce and due to these, quantity of deformed powders with a flake or laminate shape rise as shown in Figure 3(b). According to MA advances, flakes starts to overlay longitudinal axis and cold welding, obtaining particles with laminar structure and bigger size. Until now the main mechanism of the process was cold welding of particles instead of fracture. In later stages, after forming laminar particles, when collision forces are large enough to overcome particles compressive strength, together with cold welding, fracture mechanism starts to occur decreasing particles size up to 16,6 μm for 8 hours of milling as shown in Figure 3(c). In this step, the equilibrium state between both mechanisms is reached and thereby equiaxial particles start to form. In the last hours of milling, particles tends to regain the spherical shape as shown in Figure 3(d) and starts to increase in size again.

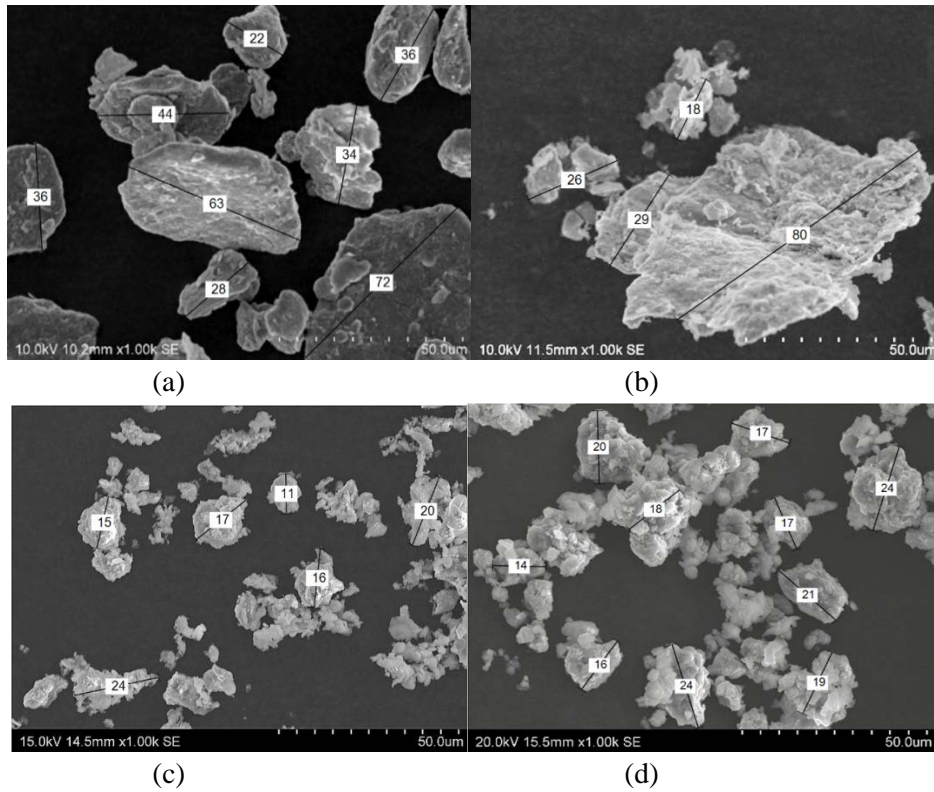


Figure 3. Morphology evolution as function of MA time: (a) 1h, (b) 4h, (c) 8h, (d) 10h.

Regarding to reinforcement distribution, for shorter times TiB_x tends to deposit on the aluminium surface and for longer times greater adhesion with aluminium matrix is achieved. Nonetheless TiB_x particles were well distributed in the matrix for both shorter and longer times as Figure 4 shows. Also the presence of reinforcement agglomerates of up to 2 μm have been determined. This effect was shown before during the base material characterization.

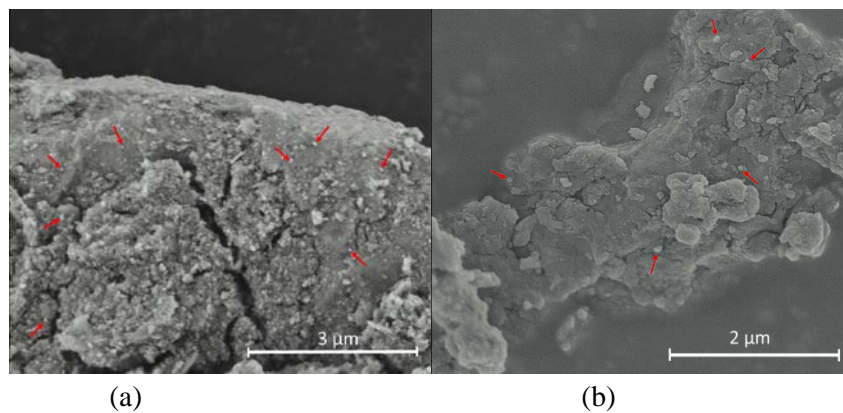


Figure 4. TiB_x nanoparticles distribution in the matrix for: (a) 1h and (b) 8h of MA.

3.3. Microstructure

The phases present in the different samples have been analysed by XRD (Figure 5). Most intense peaks correspond to aluminium main phase and less characteristic peaks refer to TiB_x reinforcement. In this case, it only can be seen TiB (not TiB_2) peaks because majority of the reinforcement correspond with this phase and the x-ray diffractometer can't detect phases below 2wt%. The peak employed to analyse crystal size, which corresponds with $(111)_{Al}$ decrease its intensity as the milling time increase. Also an increase of peaks angle is detected (moves to the right) for more hours of milling, produced by particles plastic deformation. During the first hours of MA heavy deformation is introduced into the particles. This is manifested by the increased number of grain boundaries and also by the presence of a variety of crystal defects such as dislocations or vacancies [14]. For this reason, there is a noteworthy increment of peak angle from 1 hour to 3 hours of milling.

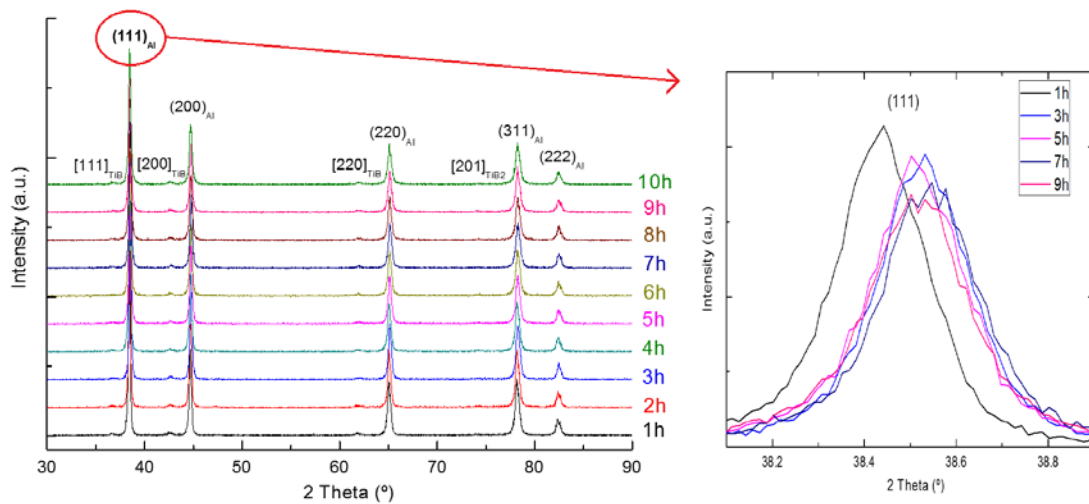


Figure 5. XRD pattern of A6005/ TiB_x powders for different MA times.

Metallographic attack was performed to see particles grain boundaries more clearly. The microstructure of the samples with 1 and 2 hours of MA can be seen in Figure 7. For longer times it was not possible to reveal the microstructure due to the high deformation that mask the grain limits. It shows an equiaxial and polycrystalline structure with a grain size around 5 μm . Both attacks reveal the presence of alloying elements as precipitates in grain boundaries.

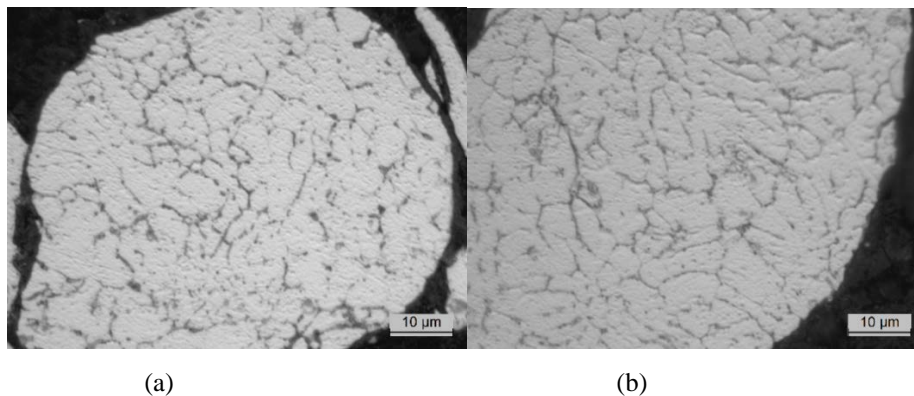


Figure 7. Composite microstructure obtained by OM: (a) 1h, (b) 2h of MA.

Figure 8 shows crystal size applying the Scherrer equation and the XRD analysis. It is observed that crystal size decreases from 44 up to 34 nm depending of milling time. As expected at longer times, less size can be obtained. This decrease in crystal size could be inversely proportional to the increase in lattice micro-strain. This effect together with peaks angle increase, could explain lattice strain increase in the first steps of the milling.

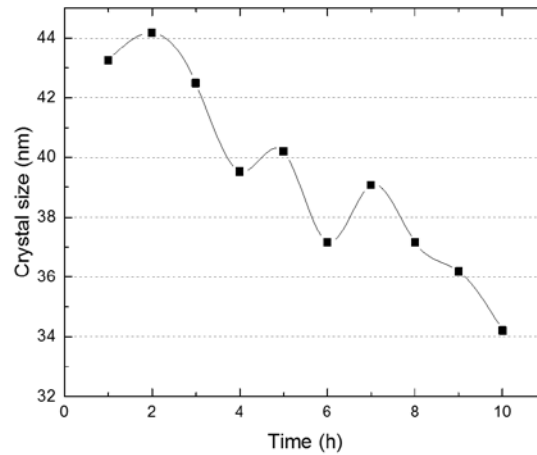


Figure 8. Crystal size in function of milling time (X-ray diffraction analysis).

3.4. Mechanical Properties

Mechanical properties of the composite were evaluated by micro-hardness tests. Figure 9 represents hardness evolution vs milling time. It tends to increase for longer times. In this case, even it reached more than double of the value from 80,1 HV for 3 hours up to 185,6 HV for 10 hours of MA. It is due to different reasons, all of them related with the increase of milling time: less size of composite powders, greater reinforcement dispersion and also hardening of the aluminium matrix itself by deformation.

Comparing Figures 8 and 9, where hardness and crystal size are related with milling time, it can show as from 7 hours for both cases, it produce a drastic decrease and increase of crystal size and hardness respectively. This confirms the direct relation between improving properties and crystal size reduction.

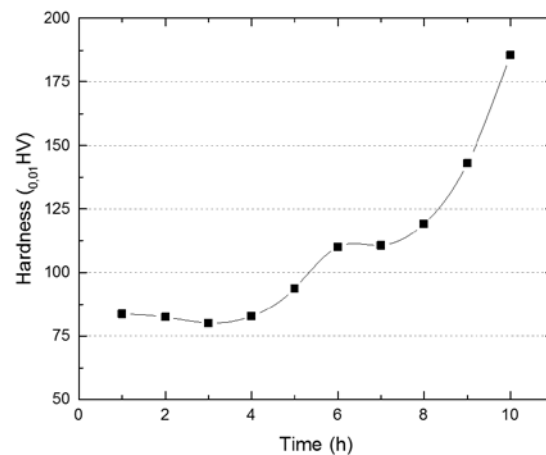


Figure 9. Micro-hardness vs milling time.

4. Conclusions

- If the composite material obtaining process is optimized employing the adequate parameters (cyclical operation mode and ball-to-powder weight ratio of 10:1), it can be achieved good reinforcement distribution and a noteworthy decrease in particle size resulting in optimum properties.
- Observing composite morphological evolution, for the first hours of MA (2 hours approximately), flakes shape particles are obtained. As the milling progresses, particles start to acquire laminar structure and in the later stages of milling, upon reaching steady state, it tends to form equiaxed particles (8 hours).
- According to MA advances, it achieves crystal refinement from 44 nm to approximately 35 nm for 10 hours of milling. Due to this results, it can be deduced how mechanical properties are directly related with crystal size and for this reason hardness also progressively increase with milling time.
- In base to these results, an optimum milling time could be around 8 hours; this time is enough to optimize the process obtaining composite powder suitable for a subsequent extrusion.

Acknowledgments

This work was supported by Ministerio de Economía y Competitividad (project MAT2013-48166-C3-3-R) and Comunidad de Madrid through the program MULTIMAT (reference S2013/MIT-2862-CM).

References

- [1] S. Hurley. MMCs find broad range of niche markets. *Met. Bull. Mon*, 54–56, 1995.
- [2] I.G. Watson, M.F. Forster, P.D.Lee, R.J. Dashwood, R.W. Hamilton, A. Chirazi. Investigation of the clustering behaviour of titanium diboride particles in aluminium. *Compos. Part A*, 36:1177–1187, 2005.
- [3] H.Ahamed, V. Senthilkumar. Role of nano-size reinforcement and milling on the synthesis of nano-crystalline aluminum alloy composites by mechanical alloying. *J. Alloys Compd.*, 505:772-782, 2010.

- [4] M. Gajewska, J. Dutkiewicz, J. Morgiel. Effect of reinforcement particle size on microstructure and mechanical properties of Al/AlN nano-composite produced using mechanical alloying. *J. Alloys Compd.*, 586:423-427, 2014.
- [5] O. Balci, D. Agaogullari, H. Gokce, I. Duman, M. Lufti Ovecoglu. Influence of TiB₂ particle size on the microstructure and properties of Al matrix composites prepared via mechanical alloying and pressureless sintering. *J. Alloys Compd.*, 586:78-84, 2014.
- [6] M. Khakbiz, F. Akhlaghi. Effect of mechanical alloying process parameters on characteristics of Al-B₄C nanocomposite-nanocrystalline powder particles. *Int. J. Mod. Phys. B*, 22:2924-2932, 2008.
- [7] E.M. Ruiz-Navas, J.B. Fogagnolo, F. Velasco, J.M. Ruiz-Prieto, L. Froyen. One step production of aluminium matrix composite powders by mechanical alloying. *Compos. Part A*, 37:2114-2120, 2006.
- [8] N. Zhao, P. Nash, X. Yang. The effect of mechanical alloying on SiC distribution and the properties of 6061 aluminium composite. *J. Mater. Process. Tech.*, 170:586-592, 2005.
- [9] C. Suryanarayana, N. Al-Aqeeli. Mechanically alloyed nanocomposites. *Prog. Mater. Sci.*, 58:412, 2013.
- [10] Z. Sadeghian, B. Lotfia, M.H. Enayatib, P. Beissc. Microstructural and mechanical evaluation of Al-TiB₂ nanostructured composite fabricated by mechanical alloying. *J. Alloys Compd.*, 509:7758-7763, 2011.
- [11] L. Kollo, M. Leparoux, C.R. Bradbury, C. Jaggi, E. Carreño-Morellic, M. Rodríguez-Arbaizarc. Investigation of planetary milling for nano-silicon carbide reinforced aluminum metal matrix composites. *J. Alloys Compd.*, 489:394-400, 2010.
- [12] A.R. Othman, A. Sardarnejad, A.K. Masrom. Effect of milling parameters on mechanical alloying of aluminum powders. *Int. J. Adv. Manuf. Tech.*, 76:1319-1332, 2015.
- [13] E.M. Ruiz-Navas, C.E. Costa, F. Velasco López, J.M. Torralba Castelló. Aleación mecánica: Método de obtención de polvos metálicos y de materiales compuestos. *Rev. Metal. Madrid*, 36:279-286, 2000.
- [14] N. Parvin, R. Assadifard, P. Safarzadeh, S. Sheibani, P. Marashi. Preparation and mechanical properties of SiC-reinforced Al6061 composite by mechanical alloying. *Mater. Sci. Eng. A*, 492:134-140, 2008.